

Unexpected variations in pulsar flux-densities at mm-wavelengths

M. Kramer¹, K.M. Xilouris², B. Rickett³

¹ Max-Planck-Institut für Radioastronomie, Auf dem Hügel 69, D-53121 Bonn, Germany

² National Astronomy and Ionospheric Center, Arecibo Observatory, P.O. Box 995, Arecibo, Puerto Rico 00613

³ Department of Electrical and Computer Engineering, University of California, San Diego, CA 92093-0407, USA

Received 8 July 1996 / Accepted 29 October 1996

Abstract. Monitoring of the flux-densities near 30 GHz are reported for four pulsars. Statistically significant variations apparently random in nature are found over 10 to 20 minutes, with rms amplitudes 20% to 100% of the mean flux. These fluctuations are substantially above the predictions for interstellar scintillation at these high frequencies. The observations presented here comprise the first attempt towards understanding the effects of the ISM on pulsar signals at such high frequencies, a spectral region where very little is known about the behaviour of pulsars or the ISM. When extrapolated from observations at lower frequencies, the four pulsars should exhibit very weak interstellar scintillation, with rms modulation indices from 2% to 14%. The fluctuations therefore are attributed rather to intrinsic variation of the pulsar emission at these frequencies.

Key words: pulsars: general – pulsars: individual: B0329+54, B0355+54, B1929+10, B2021+51 – ISM: general – radiation mechanisms: miscellaneous

1. Introduction

Apart from pulse-to-pulse modulations, pulsars are generally known to be stable radio sources (e.g. Stinebring & Condon 1990). Variations in the measured flux-density on time-scales of minutes or hours to days or months are mostly attributed to extrinsic reasons, viz interstellar scintillation. Interstellar scintillation (ISS) is caused by irregularities in the electron density, n_e , of the interstellar medium (ISM) which span scales from 10^7 – 10^{13} m (Armstrong et al. 1995). The time scale and depth of the modulations are strong functions of distance and frequency. At typical pulsar observing frequencies one distinguishes between two scintillation regimes (e.g. Rickett 1990). Small scale structures in the ISM (10^7 – 10^9 m) produce short term flux-density variations on time scales of minutes to hours, known as *Diffraction Interstellar Scintillation* (DISS, Cordes et al. 1985). Large scale structures (10^{11} – 10^{13} m) cause longer term flux-density variations on the order of days to months (Sieber 1982), known as *Refractive Interstellar Scintillation* (RISS, Rickett et

al. 1984, Kaspi & Stinebring 1992). While most of the studies have been carried out at low frequencies where pulsars are strong emitters, very few observations of ISS have been made at higher frequencies. The detection of pulsars at mm-wavelengths (Wielebinski et al. 1993) and the subsequent studies (Kramer et al. 1996; Xilouris et al. 1996; hereafter K96 and X96) motivated the present work, which aims at understanding fluctuations of pulsar signals at mm-wavelengths – an unexplored spectral region for the behaviour of the ISM.

As a wavefront from the emitted pulse passes through a region of irregularities, it suffers random perturbations in the relative phases, due to variations in the local refractive index. The scattered waves interfere at the position of a distant observer resulting in a diffractive modulation of the measured flux-density as the telescope moves through the interference pattern. These short-term DISS variations appear to be further modulated by long-term RISS variations, caused by large scale focusing or defocusing along the average path. The depth of the RISS modulations is typically lower than that of the DISS modulations. The modulation index, m , is defined as the noise corrected normalized root mean square variation in pulse flux-densities,

$$m = \frac{\sqrt{\sigma_{\text{on}}^2 - \sigma_{\text{off}}^2}}{\langle I_{\text{on}} \rangle - \langle I_{\text{off}} \rangle} \quad (1)$$

where $\langle I_{\text{on}} \rangle$ and $\langle I_{\text{off}} \rangle$ denote the mean of the measured on and off the pulse emission, respectively; σ_{on}^2 and σ_{off}^2 the corresponding variances around the mean. Whereas for DISS m is about unity, the slower RISS variations can be seen with m substantially less than unity, when the signals are averaged to suppress the DISS.

The above description applies for strong scintillation. As the frequency increases or the path length decreases, the scales of the two regimes approach each other. At a critical frequency (ν_{crit}) they merge into a single modulation at the Fresnel scale ($\sqrt{L\lambda}/2\pi$, for pulsar at distance L); for higher frequencies still, the scintillations are weak and m decreases strongly as $(\nu/\nu_{\text{crit}})^{1.42}$. The actual value of the critical frequency increases with the distance of the pulsar and is generally located at around

Send offprint requests to: M. Kramer (mkramer@mpifr-bonn.mpg.de)

a few GHz for pulsars beyond about 1 kpc (Backer 1975, Pynzar' & Shishov 1980, Malofeev et al. 1996). The observations presented here were performed in a spectral region well above the critical frequency in a regime where weak ISS prevails and therefore very weak fluctuations are expected. In the following, the observations of unexpected pulsar fluctuations are described together with the procedures taken to reduce instrumental effects.

2. Observations

We have recently performed the first study of radio pulsars at mm-wavelengths, using the 100-m Effelsberg radiotelescope of the MPIfR (Wielebinski et al. 1993, K96, X96). The data presented in this paper were obtained in December 1993 at 29.3 GHz ($\lambda 10.23\text{mm}$), in July 1994 at 32.0 GHz ($\lambda 9.37\text{mm}$) and in December 1995 at 35.4 GHz ($\lambda 8.47\text{mm}$). For the December sessions we used a tunable receiver installed in the prime focus of the telescope providing signals of one linear polarization and 2 GHz bandwidth. In the observations in July 1994 we obtained both left and right hand circularly polarized signals. Here, a receiver of fixed centre frequency was installed in the secondary focus of the telescope and also provided a bandwidth of 2 GHz. While the weather conditions during the December sessions were rather unstable, i.e. involving cloudy sky, rain and even sometimes snow, the July session was made under *near perfect and stable* weather conditions where both atmospheric and differential telescope temperature varied a few degrees along the dish surface for long sessions during night and day time. Further details of the observing system are summarized in Table 1, and also given by K96.

The received signals were sampled every $P/1024$ s and folded synchronously to the pulsar topocentric period P . Sub-integrations of 15s were stored on disk for later analysis. A noise diode, which was directly coupled into the waveguide following the antenna horn, was used as a calibration signal and was switched on synchronously to the pulse period during the first fifty phase bins of each integration. The stability of the calibration signal itself was checked during the pointing observations of well-known flux calibrators; these were made regularly after each integration on a pulsar, which lasted typically 60 to 90 min. A detailed description of the applied flux calibration scheme can be found in Kramer (1995). The calibration runs on continuum sources enabled us to monitor the gain-elevation dependence which shows that significant corrections to the measured flux-densities need to be applied when our measurements are done at very high elevations (above 70°) and very low elevations (below 20°). The data presented here were however taken at elevation between 22° and 70° (see Table 2).

3. Data analysis and results

During investigations leading to those results already presented by Wielebinski et al. (1993), K96 and X96, we noticed significant variations in the measured flux-densities observed at a particular frequency. The flux-densities varied on time scales of ten

to twenty minutes around a stable mean value which itself did not significantly differ between different observing sessions. In order to investigate these modulations further, we studied the time variability of the strongest sources. From eight pulsars detected at mm-wavelengths (K96), only PSRs B0329+54, B0355+54, B1929+10 and B2021+51 exhibited flux-densities large enough to obtain high signal-to-noise ratio measurements during short sub-integrations. Typical examples of observed flux variations are given in Figs. 1 a–d. In all figures each single measurement designated by an open circle corresponds to a sub-integration of five minutes. The plotted value always represents the *equivalent continuum flux-density*, which is the observed pulse energy averaged over one pulse period. This flux-density would be observed if the pulsar emitted the same amount of energy as a continuum source. Hereafter, quoted flux-densities always refer to this definition. The error for each measurement was derived by taking the calibration procedure into account and was estimated to be about 15 to 20 % of the mean value. The dashed horizontal line marks the average value of the continuum flux-density measured for the corresponding observation. Flux variations of a factor of two or four are clearly seen, which are much stronger than the levels of weak ISS expected at the observing frequencies. Corresponding modulation indices calculated according to Eq. (1) are quoted in Table 2 and plotted versus dispersion measure of the source in Fig. 2.

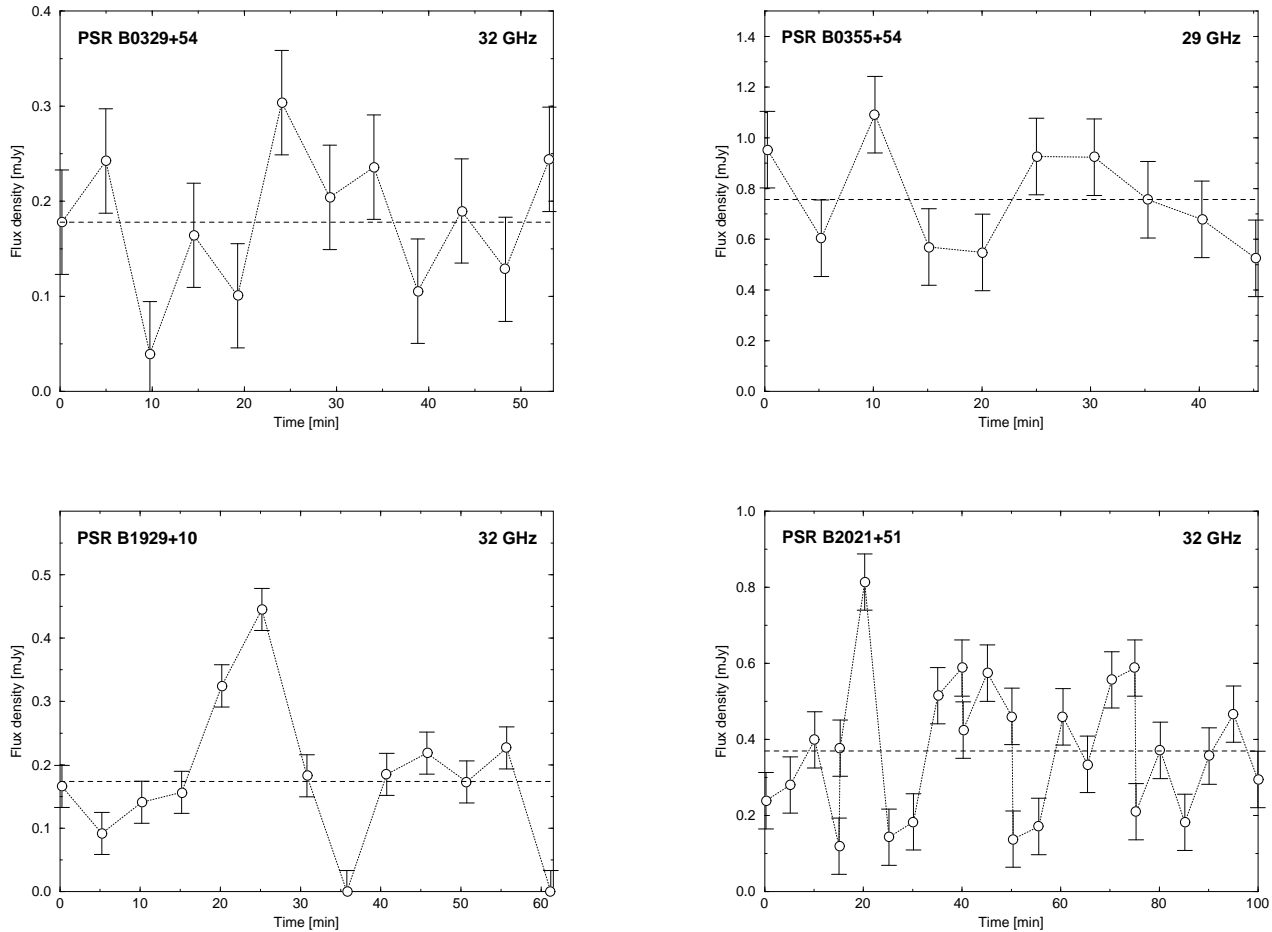
In order to minimize effects due to the measurement of only linearly polarized signals, we concentrated our analysis mainly on total power signals received at 32 GHz. Only for B0355+54, we included observations made with the tunable prime focus receiver. PSR B0355+54, being the strongest source in our sample and, thus, used as a test source, was regularly observed for short time intervals frequently interrupted by pointing and focusing runs. This prohibited a long continuous run as needed for this analysis. For all other pulsars, the analysed data represent total power signals which were obtained after adding left and right hand circularly polarized signals. We used the information provided by the calibration signal to correct for possible gain differences.

The gain stability of the system was monitored by performing the same data analysis simultaneously for on-pulse data and for the calibration signal, present in the first fifty phase bins of the pulse profile. The resulting modulation index of the calibration signal was typically $m_{cal} = 0.003$. The off-pulse power level (baseline) changed smoothly as a function of elevation due to changes in the ground illumination. This variation was subtracted from the data and the remaining calibration signal deflection was found to be stable in time. The inferred gain was found to be stable to 0.3%.

Trying to account other instrumental effects for the observed flux-density modulation, we can also consider pointing problems of the telescope, since inaccurate telescope pointing could have severely altered the measured flux-densities. We examine this effect in detail below. Observing at 32 GHz with a secondary focus receiver at the 100-m Effelsberg telescope, the HPBW becomes $25''$. Monitoring continuum sources prior and after each pulsar observing session resulted in a typical *pointing* accu-

Table 1. System parameters for observations at mm-wavelengths.

ν [GHz]	Date	T_{sys} [K]	Gain [K/Jy]	Bandwidth [GHz]	Signals
29.3	22 – Dec – 1993	120	0.37	2	linear
32.0	2/3/4 – Jul – 1994	''	''	''	LHC & RHC
35.4	20 Dec – 1994	''	''	''	linear

**Fig. 1a–d.** Variations in the flux-density observed for PSRs **a** B0329+54, **b** B0355+54, **c** B1929+10 and **d** B2021+51 at mm-wavelengths. Each single measurement (open circle) corresponds to five minutes integration. The horizontal dashed line designates the mean value of the flux-density measured for this scan.

racy of about $5''$ rms. This confirms results of routine telescope monitoring under good weather conditions (e.g. Altenhoff et al. 1980). The pointing error generally increases if large temperature gradients exist during an observing session. Differential temperature monitoring of the telescope surface, however, revealed only deviations as small as one degree. Assuming that only the largest measured flux-densities represent the “true” on-source measurement, we estimated a typical offset of the Gaussian telescope beam pattern from the actual on-source position, necessary to explain the observed flux-density variations. These calculations imply a *tracking* inaccuracy of

typically $17''$ (B0329+54), $11''$ (B0355+54), $25''$ (B1929+10) or $18''$ (B2021+51), respectively. These values are substantially larger than the typical pointing errors derived from measurements of continuum sources. Moreover, even if a large pointing error would exist, i.e. the actual pointing position of the telescope deviates from the requested one, the real *tracking* accuracy is typically better than $1''$ and thus extremely stable. Obviously, we can exclude pointing problems as the reason for the observed flux-density modulations.

As already noted, the weather conditions during the 32 GHz observations in July 1994 were extremely good, suggesting that

Table 2. Modulation indices for the four strongest sources at mm-wavelengths. We quote the dispersion measure, DM, of the pulsar (column 2), distance (column 3) observing frequency, ν (column 4), in GHz, the total observing time, T (column 5), in minutes, the average source elevation during scan (column 6) and observed modulation indices, m_{obs} (column 7). All observation were done with 2 GHz bandwidth. The predicted scintillation parameters are transition frequency (column 8), scintillation index and time scale (column 9 and 10).

PSR B	DM [cm^{-3}pc]	Dist [kpc]	ν [GHz]	T [min]	Elev.[$^\circ$]	m_{obs}	ν_c [GHz]	m_{iss}	τ_{iss} [min]
0329+54	26.8	1.43	32.0	28	64	0.5 ± 0.1	5.13	0.07	28
				48	52	0.47 ± 0.05			
0355+54	57.0	2.07	29.3	45	70	0.27 ± 0.03	7.54	0.14	68
			35.4	25	43	0.18 ± 0.01		0.11	62
1929+10	3.2	0.17	32.0	20	35	0.6 ± 0.2	1.79	0.02	17
				51	48	1.0 ± 0.4			
				61	30	0.7 ± 0.2			
2021+51	22.6	1.22	32.0	45	55	0.4 ± 0.1	3.23	0.04	37
				50	57	0.36 ± 0.06			
				55	23	0.52 ± 0.08			
				80	50	0.58 ± 0.08			
				100	50	0.48 ± 0.05			

atmospheric modulations should be negligible. As a check of atmospheric variability we examined the rms variation in the measured flux on the calibration scans, performed typically every one or two hours. Such calibration-scans consisted of cross scans on the calibrator nearest to the pulsars and lasted about two minutes, in total covering elevations between 20° and 85° . The rms deviations in observed calibrator flux-densities for the whole 72h observing period (i.e. including day and night time) were no larger than 10–15%. This confirms that the pulsar variations (seen on much shorter time scales and thus for the same atmospheric condition throughout the corresponding scan) at more than 20% are not atmospheric. Additionally, atmospheric effects should be visible in a possible dependence of the derived modulation indices on the elevation of the source during the corresponding observation (column 6 of Table 2). We plot these quantities in Fig. 3. A correlation is obviously not present, confirming that the variations are not atmospheric.

4. Discussion

Since our observations were made at very high radio frequencies, they should be representative of the weak scintillation regime (see Malofeev et al. 1996), where the flux modulation is expected to be small. Unexpectedly, we have observed *substantial* variations in the measured flux-densities. In fact averaging the observations (neglecting different integration times) we obtain mean values for the modulation indices of $m(0329 + 54) = 0.44 \pm 0.04$, $m(0355 + 54) = 0.21 \pm 0.04$, $m(1929 + 10) = 0.7 \pm 0.1$ and $m(2021 + 51) = 0.47 \pm 0.04$. It is significant that the variations in each pulsar are present whenever it is observed. Interestingly, the data plotted in Fig. 2 suggest an anti-correlation of the observed modulation index with the dispersion measure. However, the number (i.e. four) of pulsars is too small to test the significance of this result.

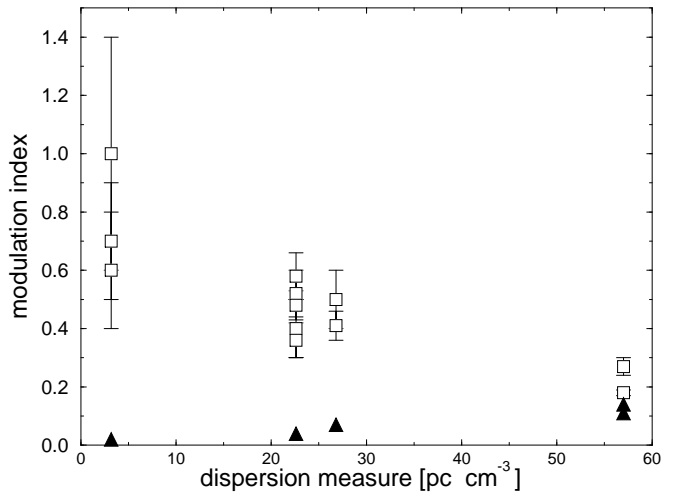


Fig. 2. Observed modulation indices, m_{obs} (open squares), and expected modulation indices, m_{iss} (filled triangles), plotted versus dispersion measure. See Table 2 and text for details.

Moreover, while the most distant pulsar B0355+54 shows only moderate modulations around a mean value of the flux-density, the other sources exhibit flux variations as large as 100% of the average value, sometimes even resulting in a non-measurable flux density during a single sub-integration. Such behaviour is *opposite* to that expected for either weak scintillation or RISS (e.g. Sieber 1982, Kaspi & Stinebring 1992, and Fig. 8b of Malofeev et al. 1996).

In order to extrapolate from low frequency ISS observations to predict ISS at our high frequencies, we assume the Kolmogorov model for the ISM density spectrum:

$$P_{\delta n_e}(q) = C_n^2 q^{-\beta}, \quad r_{\text{outer}}^{-1} < q < r_{\text{inner}}^{-1} \quad (2)$$

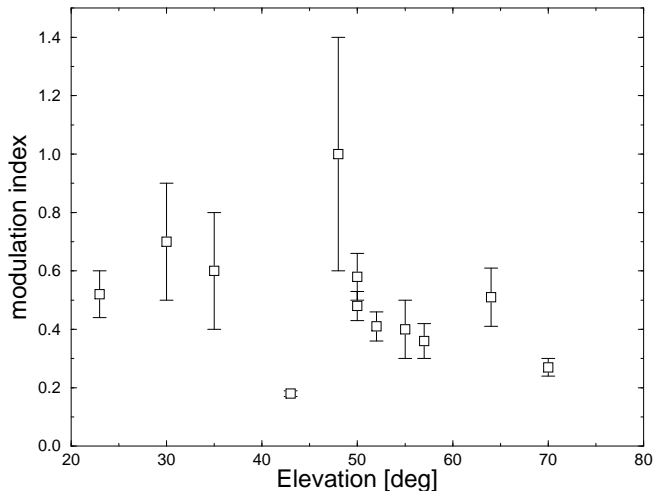


Fig. 3. Observed modulation indices plotted versus source elevation of the corresponding observation.

where q is the spatial wavenumber and C_N^2 is proportional to the mean squared electron density fluctuation along the line-of-sight (e.g. Cordes et al. 1985). Although the actual value of the power index, β , is still under discussion (see e.g. Armstrong et al. 1995, Malofeev et al. 1996), it is usually assumed that the fluctuations behave like other forms of turbulence, i.e. energy fed into large scale irregularities cascades down into smaller units of scale r_{inner} where energy is dissipated, thus heating the plasma. The resulting spectrum is that of a Kolmogorov power law with $\beta = 11/3$.

We follow Rickett (1990) and introduce a parameter, u , characterizing the strength of the ISS. At typical pulsar observing frequencies the scintillations are strong and we can define

$$u^2 \equiv \frac{\nu}{\Delta\nu_D} \quad (3)$$

where $\Delta\nu_D$ is the *decorrelation bandwidth* of the DISS, i.e. the typical frequency range over which the observed intensity is more than 50% correlated. With the Kolmogorov spectrum model, we find $u \propto \nu^{-1.7}$. In strong scintillation $u > 1$, and the decorrelation bandwidth is related to another measurable quantity, viz the pulse broadening time constant, τ_s . As scattered rays propagate different rays experience slightly different path lengths, resulting in a broadening of the pulse. The observed pulse is then a convolution of the emitted pulse by an exponentially decaying waveform of time scale τ_s . It follows that $2\pi \Delta\nu_D \tau_s = 1$ (Cordes et al. 1985). Taking observed values for τ_s scaled to 1 GHz (Taylor et al. 1993), we can calculate the strength parameter u and scale it to the observing frequency for our observations. In all cases we obtain $u < 1$, (i.e. weak scintillation), in which case Eq. (3) does not apply and $\Delta\nu_D \approx \nu$.

For weak scintillation, the modulation index is approximately given by (Rickett 1990):

$$m_{\text{iss}} \sim u^{5/6} \sim (\nu/\nu_c)^{-1.42}. \quad (4)$$

These predicted values are listed in Table 2 and plotted in Fig. 2. We have also compared the values predicted by this simple theoretical formula with extrapolations based on data obtained for these pulsars between 4.75 GHz and 10.55 GHz by Malofeev et al. (1996). They measured weak scintillation for these pulsars and found modulation indices consistent with or below the predictions based on Eq. (4). We note that the more complicated scintillation model proposed by Malofeev et al. (1996) predicts m_{iss} values that are about 20% greater than from Eq. (4), but still small compared to our observed modulation indices (see Table 2). Only for B0355+54 are the observed modulations comparable to those predicted for scintillations. If the apparent inverse correlation with dispersion measure (Fig. 2) were true, it would mean a yet unexpected propagation effect. However, given the low statistical significance of the apparent inverse correlation, being based on only four pulsars, such an effect is presently a matter for conjecture.

A further comparison can be made between the observed time scales and ISS predictions. In all four pulsars the time scale for a substantial flux variation estimated from Fig. 1 is 10–20 minutes. For B2021+51, however, variations at a 2σ -level on time scales smaller than 5 min are visible, indicating that in some cases flux density variations have not been resolved. We have listed a predicted weak ISS time scale in Table 2, using equation 2.2 of Rickett (1990). The values range from 17 minutes for B1929+10 to 68 minutes for B0355+54. Whereas the observed time scales are comparable with the shortest of these, they do not show any increase with distance.

5. Conclusions

The results of our monitoring of four pulsars at frequencies near 30 GHz indicate that strong modulations of the flux-density exist at those frequencies. The modulations ranging from 20–100% of the average flux density come as a surprise in a region where the ISM is thought to be inactive and the pulsars are fading in intensity.

While we can rule out instrumental effects for the observed flux modulations, we cannot completely exclude a propagation effect due to the ionized interstellar medium. However, the observed characteristics are inconsistent with the expected weak interstellar scintillations and, though an unexpected interstellar propagation effect cannot be ruled out, we consider propagation effects as unlikely. Therefore, we are left with the conclusion that the observed large flux variations on time scales of ten to twenty minutes are most likely of intrinsic rather than extrinsic origin. We suggest that they are inherited from the emission process and might be due to a loss of coherence also indicated by other radiation properties at mm-wavelengths (see X96, Kramer & Xilouris 1996). Actually, single pulse measurements revealed an increasing pulse-to-pulse fluctuation towards high radio frequencies (1 to 8 GHz) for some pulsars (Bartel et al. 1980, hereafter B80). Assuming that single pulse observations were possible at 32 GHz, an interesting comparison follows. We have extrapolated the strength of the fluctuations measured by B80 to 32 GHz. The values obtained are as

large as $m_{B80} = 2.12$ (B0329+54), $m_{B80} = 1.27$ (B0355+54), $m_{B80} = 4.72$ (B1929+10), and $m_{B80} = 1.32$ (B2021+51). These values are even larger than the indices presented in this work. However, the latter refer to 5 min averages instead of single pulses. Smoothing simulated sequences of single pulses exhibiting the modulation index values extrapolated from B80, to our five minutes sub-integrations, we find that the observed modulation indices are still by factors of 4 to 8 higher than expected. The tendency reported by B80 of increasing modulation after a critical frequency usually located above 1 GHz, persists at mm-wavelengths and even becomes more severe than suggested by the power law determined by B80. B80 has attributed the observed erratic nature of pulsar emission to a progressive loss of coherency with frequency, which has also been suggested by K96 as the reason for the observed apparent spectral turn-up at mm-wavelengths.

Even though the location of the emission region in pulsar magnetospheres is somewhat uncertain, most current studies (e.g. Cordes 1978, Blaskiewicz et al. 1991, Phillips 1992, X96, Kramer et al. in press) seem to indicate that the radiation is created at a distance of a few percent of the light cylinder radius in a stratified mode with higher frequencies closer to the pulsar surface (radius-to-frequency mapping, RFM). Progressively increasing plasma densities and higher magnetic fields encountered close to the stellar surface might change the physical conditions in the regions that are responsible for the high radio frequency radiation. While at low frequencies the RFM is prominent, it has been shown that towards high frequencies RFM reaches a saturation and that the emission is essentially radiated from the same magnetospheric region (X96). Changes in the environment of the emission could be reflected in the modulations that we observe.

The same changes in the environment of the emission could also be responsible for the earlier reported spectral turn-up (K96). An association between these two phenomena is naturally tempting. Perhaps, the unusual spectral behaviour of B1929+10 and B2021+51 could be explained by assuming that these pulsars were observed at maximum pulsar activity. However all our observing sessions at different epochs lasted longer than an hour. Therefore, the resulting mean value was averaged over several independent time scales of the variation. Also, within the measurement uncertainties, the average flux densities taken at different epochs appear consistent. Therefore, effects of the short time variations reported here are largely suppressed from the average spectra presented by K96. Concluding, the observed flux variations cannot account for the unusual spectral behaviour earlier reported by K96 although both phenomena may well have a common physical origin.

Summarizing, we have observed unexpected flux density variations at mm-wavelengths which seem to be intrinsic to the pulsar radio emission mechanism. Further observations from 10 to 30 GHz will be needed to answer the yet open questions about their origin. A detailed study of the frequency dependence of this new variability appears to be most promising.

Acknowledgements. We want to express our gratitude to R. Wielebinski and A. Jessner for their constant help, support and valuable advices. We thank M. Timofeev for help with the observations and D. Lorimer for his helpful comments and discussions. We are also in particular grateful to C. Salter for extremely valuable suggestions and thank an anonymous referee for helpful comments. Arecibo Observatory is operated by Cornell University under cooperative agreement with NSF. BJR acknowledges the support from the NSF under grant AST-9414144.

References

- Altenhoff W.J., Baars W.M., Downes D., et al., 1980, *AJ*, 85, 9A
 Armstrong J.W., Rickett B.J., Spangler S.R., 1995, *ApJ*, 443, 209
 Backer D.C., 1975, *A&A*, 43, 395
 Bartel N., Sieber W., Wolszczan A., 1980, *A&A*, 90, 58 (B80)
 Blaskiewicz M., Cordes J.M., Wasserman I., 1991, *ApJ*, 370, 643
 Cordes J.M., 1978, *ApJ*, 222, 1006
 Cordes J.M., Weisberg J.M., Boriakoff V., 1985, *ApJ*, 288, 221
 Kaspi V.M., Stinebring D.R., 1992, *ApJ*, 392, 530
 Kramer M., 1995, PhD-thesis, University of Bonn
 Kramer M., Xilouris K.M., 1996, to appear in Proceedings of IAU Colloq. 160, Sydney 1996: Pulsars: Problems and Progress, eds. Johnston S., Bailes M., Walker M., PASP
 Kramer M., Xilouris K.M., Jessner A., et al. 1996, *A&A*, 306, 867 (K96)
 Kramer M., Xilouris K.M., Jessner A., et al., in press
 Malofeev V.M., Shishov V.I., Sieber W., et al. 1996, *A&A*, 308, 180
 Phillips J.A., 1992, *ApJ*, 385, 282
 Pynzar' A.V., Shishov V.I., 1980, *Astron. Zh.*, 57, 1187
 Rickett B.J., 1990, *ARA&A*, 28, 561
 Rickett B.J., Coles W.A., Bourgois G., 1984, *A&A*, 134, 390
 Sieber W., 1982, *A&A*, 113, 311
 Stinebring D.R., Condon J.J., 1990, *ApJ*, 352, 207
 Taylor J.H., Manchester R., Lyne A.G., 1993, *ApJS*, 88, 529
 Wielebinski R., Jessner A., Kramer M., Gil J.A., 1993, *A&A*, 272, L13
 Xilouris K.M., Kramer M., Jessner A., et al. 1996, *A&A*, 309, 481 (X96)